

CAPS STORM-SCALE ENSEMBLE FORECASTING SYSTEM: IMPACT OF IC AND LBC PERTURBATIONS

Fanyou Kong^{1*}, Ming Xue^{1,2}, Kevin W. Thomas¹, Yunheng Wang¹,
Keith A. Brewster¹, Youngsun Jung¹,
Adam Clark⁴, Michael C. Coniglio⁴, J. Correia Jr.³,
Israel L. Jirak³, Jack Kain⁴, Steven J. Weiss³

¹Center for Analysis and Prediction of Storms, and ²School of Meteorology,
University of Oklahoma, Norman, OK 73072

³NOAA/NMS/NCEP Storm Prediction Center

⁴NOAA National Severe Storm Laboratory, Norman, OK 73072

1. INTRODUCTION

Since 2007, the Center for Analysis and Prediction of Storms at the University of Oklahoma produces realtime storm-scale ensemble forecast (SSEF) each spring season to support the NOAA Hazardous Weather Testbed (HWT) Spring Experiment (Kong et al. 2007; 2008; 2009; 2012; Xue et al. 2007; 2008; 2009; 2010). The 2013 CAPS SSEF ran from April 22 to June 7, 2013, consisting of 30 multi-model multi-physics ensemble members using three NWP model systems (WRF-ARW, COAMPS, and ARPS), with a domain covering the full continental United States with convection-allowing resolution at 4-km horizontal grid spacing. CAPS SSEF members were configured with a hybrid of initial/lateral boundary condition (IC/LBC) perturbations extracted from the operational Short-Range Ensemble Forecast (SREF) ensemble members (at 16 km grid spacing) and various combinations of physics options in microphysics, PBL and land-surface model, and radiation. As in previous years, up to 140 WSR-88D Doppler weather radar data, with both radial wind and reflectivity, and other observation data were analyzed into the SSEF members in realtime using the ARPS 3DVAR and Complex Cloud Analysis system (Gao et al. 2004; Hu et al. 2006).

This extended abstract first provides highlights to the CAPS SSEF for 2013 HWT Spring Experiment in Section 2, followed by quantitative verification results on QPF in Section 3. The impact of IC and LBC perturbations on the QPF forecast in terms of ETS skill scores and on the ensemble spread by performing a 4-day small ensemble experiment in post season using different sets of IC perturbation magnitudes and different LBC perturbation strategies in Section 4.

2. EXPERIMENT HIGHLIGHT

The CAPS 2013 Spring Program started on 22 April 2013 and ended on 7 June, encompassing the NOAA HWT 2013 Spring Experiment that was officially between 6 May and 7 June 2013. Three numerical weather models were used to produce a 30 member 48 h ensemble forecast during weekdays (Monday through Friday), initialized at 0000 UTC, covering a full-CONUS

domain, which is 10% larger than in 2012 (Figure 1) at 4 km horizontal grid spacing. Some weekend day forecasts were also performed upon request from HWT depending on weather outlook. A majority of the SSEF ensemble, 26 members out of 30 total, were produced using the Weather Research and Forecast (WRF) Advanced Research WRF core (ARW), one was produced using the Advanced Regional Prediction System (ARPS), and three were produced using the Navy COAMPS model. The WRF ARW is the V3.4.1 release, with CAPS modifications that added some diagnostic quantities that HWT scientists requested. In a change from previous years, the Nonhydrostatic Mesoscale Model (NMM) was removed from the CAPS SSEF system in 2013.

Tables 1 and 2 are member configurations for ARW and ARPS (COAMPS configuration is not shown in this extended abstract). *cn* refers to the control member, with radar data analysis, *c0* is the same as *cn* except for no radar data was analyzed in. *m3 – m15* are members with both IC/LBC perturbation and physics variations, while *cn*, *c0*, and *m16 – m26* are members without IC and LBC perturbation but only physics variations. NAMA and NAMf refer to the 12 km NAM analysis and forecast, respectively. ARPSa refers to analysis after ARPS 3DVAR and Cloud Analysis using NAMA as the background.

For the ARPS model group, only *cn* member was run in the 2013 season. For the COAMPS model group, three members, *cn*, *c1*, and *c2* were configured, with the COAMPS default microphysics, the newly CAPS added Milbrandt-Yau two-moment microphysics (Milbrandt and Yau 2006a, 2006b), and a new Thompson scheme, respectively..

A new 1200 UTC initiation 8-member (WRF-ARW only) ensemble, with 18-h forecast, was produced the same way but run on a local computer system, the University of Oklahoma Supercomputing Center for Education and Research (OSCER) *Boomer* Xeon64-Oct Core Linux Cluster. The members in this 1200 UTC ensemble were configured the same as *arw_cn*, *arw_m4*, *arw_m5*, *arw_m7*, *arw_m8*, *arw_m12*, *arw_m13*, and *arw_m14* from the 0000 UTC ensemble listed in Table 1.

All 00Z forecasts used NAM 12 km (218 grid) 00Z analyses as background for initialization, with the initial condition perturbations for the perturbed ensemble members coming from the 21Z NCEP Short-Range Ensemble Forecast (SREF) 3-h forecasts. The 12Z forecasts used 12Z NAM analysis and the 09Z SREF 3-

*Corresponding Author Address: Dr. Fanyou Kong,
Center for Analysis and Prediction of Storms, Univ. of
Oklahoma, Norman, OK 73072; e-mail: fkong@ou.edu

h forecasts, respectively. The lateral boundary conditions for the 00Z ensemble came from the corresponding 21Z SREF forecasts directly for those perturbed members and from the 00Z 12 km NAM forecast for the non-perturbed members, while for the 12Z ensemble the 09Z SREF and 12Z NAM forecasts were used respectively.

For all but one member, full-resolution radar data from the nationwide WSR-88D radar network (both reflectivity and radial wind) were analyzed into the ICs using the ARPS 3DVAR and Complex Cloud Analysis package (Gao et al. 2004; Hu et al. 2006). One member from ARW model (*arw_c0*) was run without radar data analysis.

Synthetic GOES satellite brightness temperatures for the 6.48 μm and 10.7 μm infrared channels were computed using CRTM from JCSDA. New in 2013 is the production of simulated dual polarimetric Doppler radar parameters (REF, ZDR, KDP) using the CAPS dual-pol radar simulator (Jung et al. 2008; 2010).

All 0000 UTC 4 km ensemble forecasts were performed on *Darter*, a brand new Cray XC30 supercomputer system with 12,000 computing cores, at the NSF sponsored National Institute of Computational Sciences (NICS) at the University of Tennessee. This allows the entire forecasts – 30 ensemble runs at 4 km grid to use 8,500 cores in dedicated mode overnight for

about 7.5 h. Hourly model outputs were archived on the mass storage HPSS at NICS.

A total of 37 days of complete ensemble forecasts from the 00Z runs and 26 days from the 12Z runs were produced during the experiment period. Using the NSSL 1-km resolution NWQ QPE data (Zhang et al. 2011) as a verification dataset, the SSEF QPF and probabilistic QPF performance has been evaluated using various traditional verification metrics and compared to the operational 12-km NAM forecasts and the Short-Range Ensemble Forecast (SREF) products.

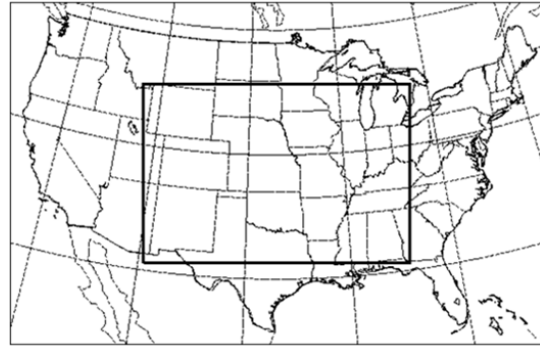


Figure 1. Model forecast domains for the 2013 Season (outer domain: 1200×768). The small inner domain (600×400) is for the experimental EnKF ensemble.

Table 1. Configurations for ARW members. NAMA and NAMf refer to the 12 km NAM analysis and forecast, respectively. ARPSa refers to ARPS 3DVAR and cloud analysis

Member	IC	BC	Radar data	Microphysics	LSM	PBL
<i>arw_cn</i>	00Z ARPSa	00Z NAMf	yes	Thompson	Noah	MYJ
<i>arw_c0</i>	00Z ARPSa	00Z NAMf	no	Thompson	Noah	MYJ
<i>arw_m3</i>	<i>arw_cn</i> + em-p1_pert	21Z SREF em-p1	yes	Morrison	RUC	YSU
<i>arw_m4</i>	<i>arw_cn</i> + nmm-n2_pert	21Z SREF nmm- n2	yes	Morrison	Noah	MYJ
<i>arw_m5</i>	<i>arw_cn</i> + em-n2_pert	21Z SREF em-n2	yes	Thompson	Noah	ACM2
<i>arw_m6</i>	<i>arw_cn</i> + nmmb-p2_pert	21Z SREF nmmb-p2	yes	M-Y	RUC	ACM2
<i>arw_m7</i>	<i>arw_cn</i> + nmm-p1_pert	21Z SREF nmm- p1	yes	Morrison	Noah	MYNN
<i>arw_m8</i>	<i>arw_cn</i> + nmmb-n1_pert	21Z SREF nmmb-n1	yes	WDM6	RUC	MYJ
<i>arw_m9</i>	<i>arw_cn</i> – nmmb-p1_pert	21Z SREF nmmb-p1	yes	M-Y	Noah	YSU
<i>arw_m10</i>	<i>arw_cn</i> + em-n1_pert	21Z SREF em-n1	yes	WDM6	Noah	QNSE
<i>arw_m11</i>	<i>arw_cn</i> – em-p2_pert	21Z SREF em-p2	yes	M-Y	Noah	MYNN
<i>arw_m12</i>	<i>arw_cn</i> – nmmb-n3_pert	21Z SREF nmmb-n3	yes	WDM6	Noah	YSU
<i>arw_m13</i>	<i>arw_cn</i> – nmmb-p3_pert	21Z SREF nmmb-p3	yes	Thompson	Noah	YSU
<i>arw_m14</i>	<i>arw_cn</i> – em-p3_pert	21Z SREF em-p3	yes	Thompson	Noah	MYNN

arw_m15	arw_cn – nmm-p2_pert	21Z SREF nmm- p2	yes	Morrison	Noah	QNSE
arw_m16	00Z ARPSa	00Z NAMf	yes	Thompson	Noah	MYNN
arw_m17	00Z ARPSa	00Z NAMf	yes	Thompson	Noah	ACM2
arw_m18	00Z ARPSa	00Z NAMf	yes	Thompson	Noah	YSU
arw_m19	00Z ARPSa	00Z NAMf	yes	Thompson	Noah	QNSE
arw_m20	00Z ARPSa	00Z NAMf	yes	M-Y	Noah	MYJ
arw_m21	00Z ARPSa	00Z NAMf	yes	Morrison	Noah	MYJ
arw_m22	00Z ARPSa	00Z NAMf	yes	WDM6	Noah	MYJ
arw_m23	00Z ARPSa	00Z NAMf	yes	NSSL	Noah	MYJ
arw_m24	00Z ARPSa	00Z NAMf	yes	Thompson	RUC	MYNN
arw_m25	00Z ARPSa	00Z NAMf	yes	Thompson +mod RRTMG	Noah	MYJ
arw_m26	00Z ARPSa	00Z NAMf	yes	WSM6	Noah	MYJ

* For all members: ra_lw_physics= RRTMG; ra_sw_physics=RRTMG; cu_physics= NONE. Member m25 uses Thompson modified RRTMG in coupled mode for both sw and lw radiations. Member m26 with WSM6 is for EnKF LBC purpose.

Table 2. Configurations for each individual member with ARPS*

member	IC	BC	Radar data	Microphysics.	radiation	sf_phy
arps_cn	00Z ARPSa	00Z NAMf	yes	Lin	Chou/Suarez	Force-restore

* For all members: no cumulus parameterization

A major new addition in the CAPS 2013 Spring Experiment was an experimental EnKF-based forecasting over a smaller central US domain which is a ¼ of the CONUS size (see Figure 1). In order to provide an ensemble background for EnKF, a separate 4-km ensemble of 9-h forecasts, starting at 1800 UTC, with 40 WRF-ARW members was produced over the CONUS domain. This ensemble was configured with initial perturbations and mixed physics options to provide input for EnKF analysis. Each member used WSM6 microphysics with different parameter settings. Table 3 lists the member configuration detail. No radar data was analyzed for this set of runs. All members also included random perturbations with recursive filtering of ~20 km horizontal correlations scales, with relatively small perturbations (0.5K for potential temperature and 5% for relative humidity).

A one-time EnKF analysis, with all available Doppler weather radar as well as conventional (sounding, profile, and surface) data, was performed at 00 UTC over the small central US domain, using the 6-h forecasts from the 40-member ensemble in Table 3. The CAPS developed EnKF package was used (Tong and Xue 2005; Xue et al. 2006; Wang et al. 2013). A 24-h forecast followed using the ensemble mean of the EnKF

analysis, with LBCs from the CONUS domain WSM6 member (m26 in Table 1). A single forecast over the same central US domain was also run using regular 3DVAR analysis over the 40-member ensemble mean forecast for comparison. Preliminary analysis of the forecast performance of this experimental EnKF ensemble set can be found in Jung et al. (2013).

3. ENSEMBLE PRODUCTS AND VERIFICATIONS

Storm-scale ensemble products were generated from a 15-member sub-ensemble that consists of the multi-model, multi-physics, IC and LBC perturbation, and radar analysis members (labeled in red in Tables 1 and 2). Post-processed products include ensemble mean and maximum, probability matched mean (Ebert 2001) of precipitation and reflectivity, frequency-based ensemble probability, and neighborhood probability of 1-h, 3-h and 6-h accumulated precipitation, reflectivity, environmental fields such as surface temperature, dew point, maximum updraft speed and maximum 10-m wind speed, CAPE-shear parameters, and storm-attribute parameters such as updraft helicity, updraft speed, and integrated graupel. The post-processed ensemble products were made available in real-time in GEMPAK

format data files to SPC and NSSL, and on the web for the HWT participants and public to evaluate. CAPS also maintains a demonstration web page to show in realtime a selected set of ensemble product¹.

Model simulated radar reflectivity was computed within each individual microphysics algorithm with consistent microphysics parameter setting to the corresponding individual scheme. For the WRF-ARW

members, special procedures were taken for all two-moment microphysics schemes used in 2013 to properly initialize number concentration when initial hydrometeor variables were present due to the Cloud Analysis. There were six microphysics schemes used in 2013. They are Thompson, Milbrandt-Yau, Morrison, WDM6, NSSL, and WSM6. The first five are partial or full two moment schemes, whereas WSM6 is a single moment scheme which was used for providing lateral boundary condition for the experimental EnKF ensemble.

¹ <http://forecast.caps.ou.edu/>

Table 3. Configuration for the EnKF ensembles

Member	IC	BC	Microphy – WSM6 (N0r, N0g, ρg)*	LSM	PBL
enk_m1	18Z ARPSa	18Z NAMf	(8,6),(4,6),500	Noah	MYJ
enk_m2	arw_cn + em-p1_pert	18Z SREF em-p1	(8,6),(4,6),500	Noah	YSU
enk_m3	arw_cn + nmm-n2_pert	18Z SREF nmm-n2	(9,4,6),(5,4),673	Noah	MYJ
enk_m4	arw_cn + em-n2_pert	18Z SREF em-n2	(2.4,7),(5.7,4),666	Noah	ACM2
enk_m5	arw_cn + nmmb-p2_pert	18Z SREF nmmb-p2	(3.7,7),(6.3,4),659	Noah	ACM2
enk_m6	arw_cn + nmm-p1_pert	18Z SREF nmm-p1	(2.5,6),(8,4),652	Noah	MYNN
enk_m7	arw_cn + nmmb-n1_pert	18Z SREF nmmb-n1	(2.6,7),(9,4),645	Noah	MYJ
enk_m8	arw_cn – nmmb-p1_pert	18Z SREF nmmb-p1	(6.8,6),(1,5),638	Noah	YSU
enk_m9	arw_cn + em-n1_pert	18Z SREF em-n1	(3,6),(1.1,5),631	Noah	QNSE
enk_m10	arw_cn – em-p2_pert	18Z SREF em-p2	(8.4,6),(1.3,5),624	Noah	MYNN
enk_m11	arw_cn – nmmb-n3_pert	18Z SREF nmmb-n3	(1.5,7),(1.4,5),617	Noah	MYJ
enk_m12	arw_cn – nmmb-p3_pert	18Z SREF nmmb-p3	(3.1,6),(1.6,5),610	Noah	YSU
enk_m13	arw_cn – em-p3_pert	18Z SREF em-p3	(8.6,5),(1.8,5),603	Noah	ACM2
enk_m14	arw_cn – nmm-p2_pert	18Z SREF nmm-p2	(4.6,6),(2,5),596	Noah	QNSE
enk_m15	arw_cn + em-p1_pert	18Z SREF em-p1	(1.3,7),(2.2,5),589	Noah	MYNN
enk_m16	arw_cn + nmm-n2_pert	18Z SREF nmm-n2	(5.1,6),(2.5,5),582	Noah	ACM2
enk_m17	arw_cn + em-n2_pert	18Z SREF em-n2	(8.1,5),(2.8,5),575	Noah	MYJ
enk_m18	arw_cn + nmmb-p2_pert	18Z SREF nmmb-p2	(1.9,6),(3.2,5),568	Noah	ACM2
enk_m19	arw_cn + nmm-p1_pert	18Z SREF nmm-p1	(3.9,7),(3.6,5),561	Noah	MYJ
enk_m20	arw_cn + nmmb-n1_pert	18Z SREF nmmb-n1	(2.2,6),(4,5),554	Noah	QNSE
enk_m21	arw_cn – nmmb-p1_pert	18Z SREF nmmb-p1	(8.5,6),(4.5,5),547	Noah	MYJ
enk_m22	arw_cn + em-n1_pert	18Z SREF em-n1	(1.1,7),(5,5),540	Noah	MYJ

enk_m23	arw_cn – em-p2_pert	18Z SREF em-p2	(8.1,5),(5.7,5),533	Noah	YSU
enk_m24	arw_cn – nmmb-n3_pert	18Z SREF nmmb-n3	(1,7),(6.4,5),526	Noah	QNSE
enk_m25	arw_cn – nmmb-p3_pert	18Z SREF nmmb-p3	(2.2,7),(7.1,5),519	Noah	MYNN
enk_m26	arw_cn – em-p3_pert	18Z SREF em-p3	(7.2,6),(8,5),512	Noah	MYJ
enk_m27	arw_cn – nmm-p2_pert	18Z SREF nmm-p2	(8.9,6),(9,5),505	Noah	YSU
enk_m28	arw_cn – nmmb-p3_pert	18Z SREF nmmb-p3	(2.9,7),(1,6),498	Noah	ACM2
enk_m29	arw_cn – em-p3_pert	18Z SREF em-p3	(1.1,7),(1.1,6),491	Noah	QNSE
enk_m30	arw_cn – nmm-p2_pert	18Z SREF nmm-p2	(9.6,6),(1.3,6),484	Noah	MYJ
enk_m31	arw_cn + em-p1_pert	18Z SREF em-p1	(3.1,6),(1.4,6),477	Noah	QNSE
enk_m32	arw_cn + nmm-n2_pert	18Z SREF nmm-n2	(1.3,6),(1.6,6),470	Noah	MYNN
enk_m33	arw_cn + em-n2_pert	18Z SREF em-n2	(2,6),(1.8,6),463	Noah	MYJ
enk_m34	arw_cn + nmmb-p2_pert	18Z SREF nmmb-p2	(4.4,6),(2,6),456	Noah	YSU
enk_m35	arw_cn + nmm-p1_pert	18Z SREF nmm-p1	(1.7,6),(2.2,6),449	Noah	ACM2
enk_m36	arw_cn + nmmb-n1_pert	18Z SREF nmmb-n1	(4.3,6),(2.5,6),442	Noah	QNSE
enk_m37	arw_cn – nmmb-p1_pert	18Z SREF nmmb-p1	(1.3,6),(2.8,6),435	Noah	MYNN
enk_m38	arw_cn + em-n1_pert	18Z SREF em-n1	(9.1,5),(3.2,6),428	Noah	MYJ
enk_m39	arw_cn – em-p2_pert	18Z SREF em-p2	(5,6),(3.6,6),421	Noah	YSU
enk_m40	arw_cn – nmmb-n3_pert	18Z SREF nmmb-n3	(6.1,6),(3.9,6),414	Noah	MYJ

* For N0r and N0h, (a, b) are coefficients of $a \times 10^b$.

Using the NSSL National Mosaic Multi-Sensor quantitative precipitation estimation (QPE) or NMQ (Zhang et al. 2011) as verification dataset, the QPF data from the 0000 UTC CAPS SSEF have been verified. The NMQ has 1-km resolution data available in 5 min interval. They were first interpolated to the 4-km SSEF grid using bilinear interpolation. 1200 UTC ensemble forecasts, as well as the experimental EnKF ensemble were not analyzed in this extended abstract.

Figure 2 shows the equitable threat scores (ETS) for the 3-hourly accumulated precipitation from the 15 base ensemble members (marked red in Tables 1 and 2) along with the ensemble mean and the probability matched mean (PM) (Ebert 2001; Clark et al. 2009; Kong et al. 2008), averaged over all 2013 SSEF forecasts (a total 37 dates of complete 0000 UTC SSEF forecasts). The ETS scores from the operational 12-km NAM forecasts, interpolated to the same 4-km CONUS grid, are also presented for comparison. Benefitting from a removal of a hidden bug in the initial perturbation generation code in ARPS that was introduced prior to

2012 CAPS Spring Experiment season which led to unreasonable behavior for the perturbed members (Kong et al. 2012), the ETS scores from the 2013 forecasts in Figure 2 exhibit good degree of spread among members and PM shows clear outscoring against individual members and simple ensemble means (mn). It, along with most SSEF members, also outperforms the operational NAM by a wide margin.

The ETS scores of 3-h accumulated precipitation from all WRF-ARW members are plotted in Figure 3, grouped into two categories of perturbed (PERT) and non-perturbed (PHY) members. Here, perturbation is refers to initial condition (IC) and lateral boundary (LBC) perturbations. As expected, it shows that the PHY ensemble (red lines) has a narrower spread compared to PERT members (black lines), especially in Figure 3a. However, it is quite surprising to see that the PHY members, at least for the low threshold (Figure 3a), generally score higher than the PERT members. This is less obvious in the higher threshold in Figure 3b. We suspect the magnitude of initial perturbations may

contribute to the somewhat lower ETS scores for the perturbed members. A set of post season rerun experiments was performed to further study this in next section.

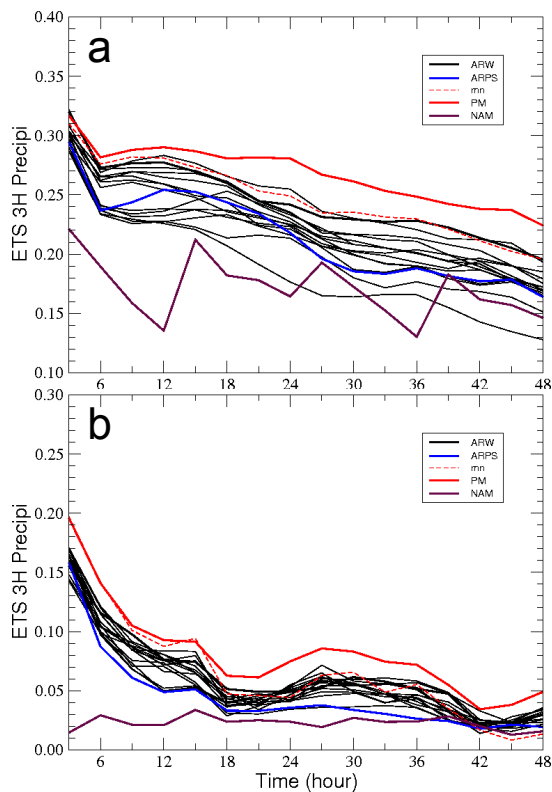


Figure 2. ETS of 3-hourly accumulated precipitation ≥ 0.01 inch (a) and 0.5 inch (b), averaged over all 2013 CAPS SSEF forecasts initiated at 0000 UTC.

4. IMPACT OF IC AND LBC PERTURBATIONS

4.1 Experiment design

To further investigate why the perturbed sub-ensemble underscores non-perturbed sub-ensemble (in Figure 3) in terms of QPF ETS, and generally examine the impacts of different IC/LBC perturbation strategies on QPF skill and ensemble characteristics, a set of reruns was performed in post season over the same CONUS domain. The perturbed members (PERT) include *m03* – *m15* in Table 1, while the non-perturbed members (PHY) are those highlighted in gray in Table 1. Table 4 lists the experiment settings. Four case dates were rerun. They include the May 15, 19, 20, and 21 cases, all dates with active convection.

In Table 4, experiments *pert_2.0* and *phys* are essentially the realtime Spring Experiment setting, referring to PERT and PHY members, respectively (in Table 1 and Figure 3). *pert_2.0* refers to the amplitude scale factor of 2.0 was used for IC perturbations, representing perturbation amplitudes of 2.0 m/s for *u* and *v*, 1.0 K for potential temperature, 0.5 g/kg for specific humidity, respectively.

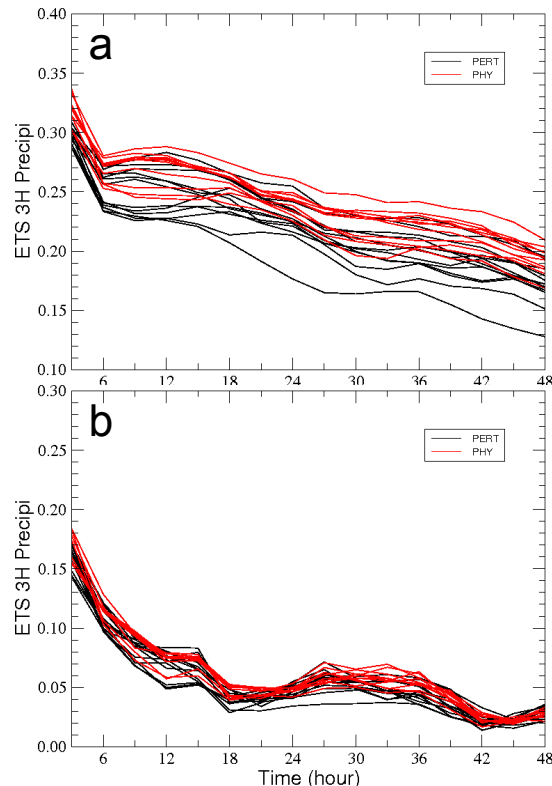


Figure 3. ETS of 3-h accumulated precipitation ≥ 0.01 inch (a) and 0.5 inch (b) from ARW members, averaged over all 2013 CAPS SSEF forecasts initiated at 0000 UTC. PERT (black) and PHY (red) refer to ARW perturbed members and physics only (non-perturbed) members, respectively.

Three experiments were configured the same as *pert_2.0* but with decreased initial perturbation amplitude scale factors (*pert_1.0*, *pert_0.5*, *pert_0.0*) where *pert_0.0* does not have IC perturbation at all as in *phys*. Another experiment, Experiment *Fix_LBC* was configured the same as *pert_2.0* in IC but with a single NAM LBC as in *phys*.

Table 4. IC/LBC perturbation experiment setting

Experiment	IC perturbation amplitude	LBC perturbation
<i>pert_2.0</i> (full_2.0)	2.0	SREF LBC
<i>pert_1.0</i>	1.0	SREF LBC
<i>pert_0.5</i>	0.5	SREF LBC
<i>pert_0.0</i>	0.0	SREF LBC
<i>Fix_LBC</i>	2.0	NAM LBC
<i>phys</i>	0.0	NAM LBC
<i>Ext_LBC</i>	2.0	extracted

What LBC perturbation strategy should be used is another topic of interest in this study. For the CAPS realtime SSEF in the Spring Experiment, the LBCs for each individual perturbed member were directly

downscaled from the corresponding SREF perturbed member. Experiments *pert_2.0*, *pert_1.0*, *pert_0.5*, and *pert_0.0* in Table 4 all employ this strategy. A second LBC strategy was tested in an additional experiment, in which the LBC perturbations were first extracted by subtracting the corresponding SREF perturbed member to its control member and then were added to the NAM LBC. This run is referred as Experiment *ext_LBC* for extracted LBC, while the Experiment *pert_2.0* is also referred as *dir_LBC* for direct LBC in later discussion for easy comparison.

4.2 Impact of IC perturbation amplitude on QPF scores

Figure 4 shows the ETS scores of 3-h accumulated precipitation ≥ 0.01 inch for experiments *pert_2.0*,

pert_1.0, *pert_0.5*, and *pert_0.0*, all with the same set of SREF LBC (which was perturbed) but different IC perturbation amplitudes, along with the *phys* members. All *pert_** members are referred as PERT and *phys* members are referred as PHY in Figure 4, respectively. As it can be seen from Figure 4, decreasing IC perturbation amplitude does help raise the ETS scores to match the non-perturbation (PHY) ensemble. One should note that the red lines (PHY) in all four panels in Figure 4 are the same, representing the same *phys* ensemble. This result suggests that higher IC perturbation amplitudes may lead to deterioration of QPF skills, and conversely, lowering IC perturbation amplitudes, even approaching to zero amplitude, QPF skills may be improved.

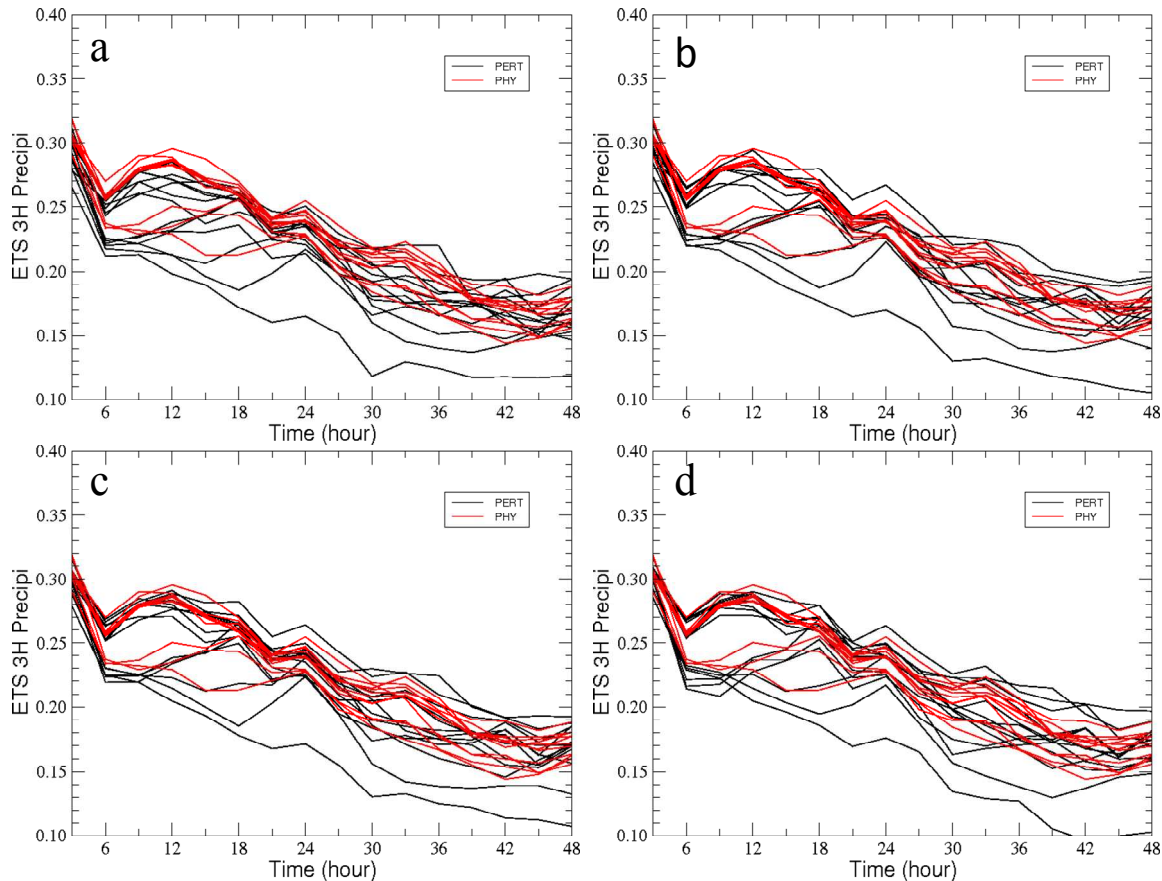


Figure 4. ETS of the 3-hourly accumulated precipitation ≥ 0.01 inch averaged over four forecast dates of May 15, 19, 20, and 21, 2013, for experiments (a) *pert_2.0*, (b) *pert_1.0*, (c) *pert_0.5*, and (d) *pert_0.0*, all with SREF LBC perturbations.

4.3 IC/LBC perturbation impact on spread

From Figures 3 and 4 it is clear that PERT and PHY ensembles have different degrees of ensemble spread or dispersion, measured as standard deviations of the ensembles. The ensemble spreads, averaged over the four rerun dates and over the entire domain grids from each of the first six experiments (in Table 4) are plotted in Figure 5, in which *full_2.0*, *1.0*, *0.5*, and *0.0* refer to Experiments *pert_2.0*, *pert_1.0*, *pert_0.5*, and *pert_0.0*, respectively. The following findings can be drawn from Figure 5:

- 1) Ensembles with IC (initial condition) and LBC (lateral boundary condition) perturbations derived from regional or global ensemble have much larger spread than physics-only ensembles;
- 2) LBC perturbations play a key role in maintaining large ensemble spread for the length of the forecast. It is interesting to see that even zero IC perturbation but full LBC perturbation (as with *pert_0.0*) shows a good degree of spread growth after 12 h into forecast, though the spread is initially lower than non-zero IC perturbations; and

3) IC perturbation alone without perturbed LBCs (*Fix_LBC*) does help increase of spread to some degree.

level except the former has narrower spread (figure not shown).

4.4 Two LBC perturbation strategies

The domain averaged ensemble spread from the two ensembles using different strategies for deriving LBC perturbations, one directly driven by corresponding SREF perturbed members (*dir_LBC*) and another with extracted perturbations from the corresponding SREF perturbed members adding to the NAM LBC (*ext_LBC*), are shown in Figure 6 along with Experiments *phys* and *fix_LBC*. *dir_LBC* is a different name of Experiment *pert_2.0*, also labeled as *full_2.0* in Figure 5.

It can be seen from Figure 6 that between the two ensembles that have same IC perturbation, the ensemble with extracted LBC perturbation has less spread than the one directly driven with SREF perturbed members. The difference is significant for 500 hPa geopotential height and mean sea level pressure. Not surprisingly, the spread of *ext_LBC* is higher than *fix_LBC*. For *ext_LBC* and *dir_LBC* ensembles, the ETS scores of 3-h accumulated precipitation are in the same

5. SUMMARY

The CAPS storm-scale ensemble forecasts (SSEF) from the NOAA HWT 2013 Spring Experiment has been evaluated against the NSSL multi-sensor QPE dataset. Probability matched mean (PM) QPF outcores individual members in terms of ETS scores, and most SSEF members outperform the operational NAM by wide margins.

Ensembles with IC and LBC perturbations derived from NCEP SREF ensemble, in addition to physics diversity, have much larger spread than physics-only ensembles. Among the IC and LBC perturbations, the latter (i.e., LBC perturbations) play key role in maintaining large ensemble spread growth. The experiments also suggest that lower IC perturbation amplitude can improve QPF skill scores, whereas higher IC perturbation amplitude may have a negative impact to the skill, even though it produces greater spread.

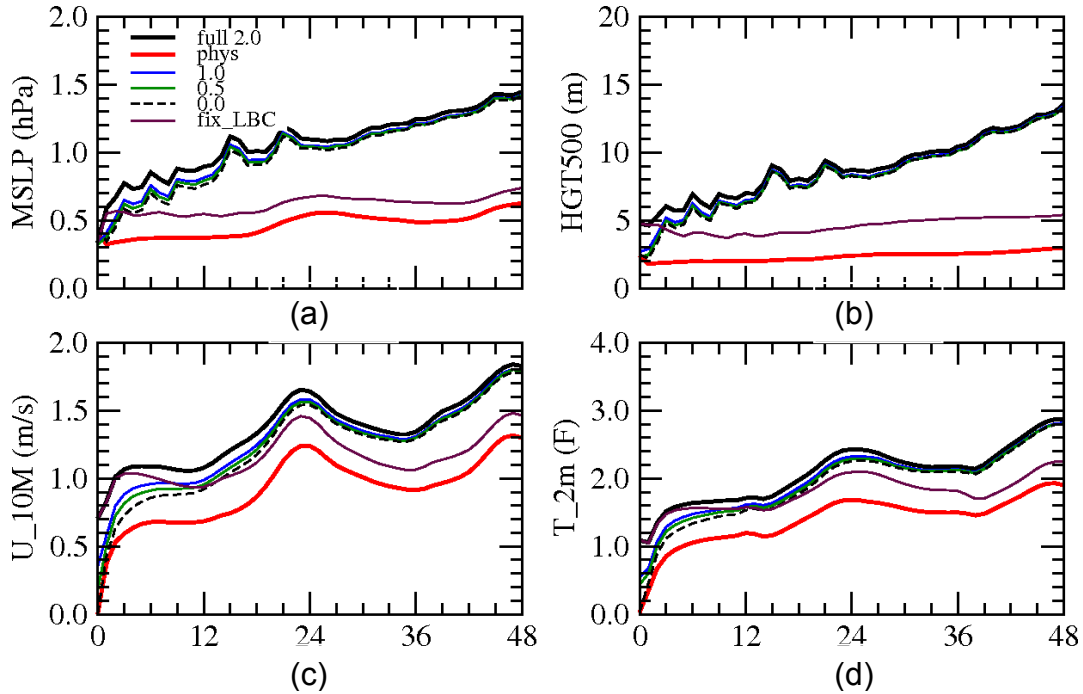


Figure 5. Domain mean ensemble spread averaged from four forecast dates of May 15, 19, 20, and 21, 2013, for all six experiments listed in Table 4. (a) mean sea level pressure (hPa), (b) 500 hPa geopotential height (m), (c) 10-m wind component *u* (m/s), and (d) 2-m temperature ($^{\circ}$ F).

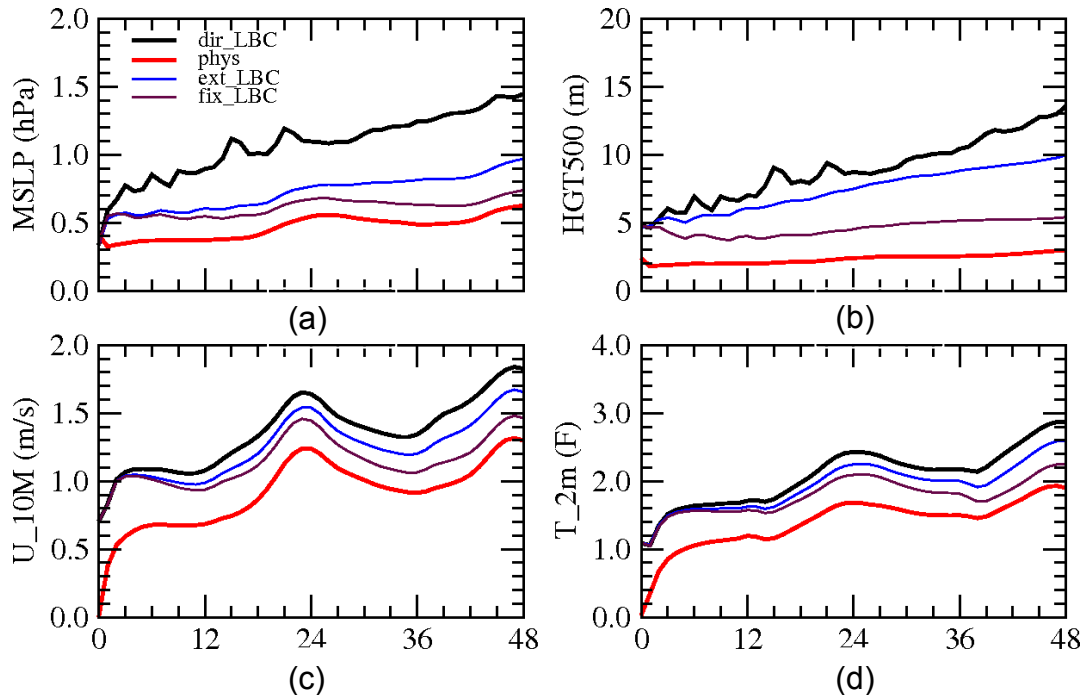


Figure 6. Same as Figure 5, but for Experiments pert_2.0 (dir_LBC), phys, fix_LBC, and ext_LBC.

Comparisons of two LBC perturbation strategies indicate that the ensemble directly driven using SREF perturbed members has higher dispersion than the ensemble with extracted LBC perturbations added to the NAM LBC. One should be mindful that no rescaling was applied to extracted LBC perturbation in this study.

Acknowledgements

This project is mainly funded by a grant from the NOAA Collaborative Science, Technology, and Applied Research (CSTAR) program (NA10NWS4680001), with other support from the NOAA GOES-R program. Most of the storm-scale ensemble forecasting runs were performed on Darter in the National Institute of Computational Sciences (NICS) at the University of Tennessee as part of the national XSEDE supercomputing allocation, part of post processing tasks and all 1200 UTC sub-ensemble forecasting jobs were performed on Boomer in the Oklahoma Supercomputer Center for Education and Research (OSCER) at the University of Oklahoma. Dr. Jun Du of NWS/NCEP provided advice and support on the SREF dataset.

6. REFERENCES

Clark, A. J., W. A. Gallus, Jr., M. Xue, and F. Kong, 2009: A comparison of precipitation forecast skill between small convection-permitting and large convection-parameterizing ensembles. *Wea. Forecasting*, **24**, 1121-1140.

Ebert, E. E., 2001: Ability of a poor man's ensemble to predict the probability and distribution of precipitation. *Mon. Wea. Rev.*, **129**, 2461-2480.

Gao, J.-D., M. Xue, K. Brewster, and K. K. Droegemeier, 2004: A three-dimensional variational data analysis

method with recursive filter for Doppler radars. *J. Atmos. Ocean. Tech.*, **21**, 457-469.

- Hu, M., M. Xue, J. Gao, and K. Brewster, 2006: 3DVAR and cloud analysis with WSR-88D level-II data for the prediction of Fort Worth tornadic thunderstorms. Part II: Impact of radial velocity analysis via 3DVAR. *Mon. Wea. Rev.*, **134**, 699-721.
- Jung, Y., G. Zhang, and M. Xue, 2008: Assimilation of simulated polarimetric radar data for a convective storm using ensemble Kalman filter. Part I: Observation operators for reflectivity and polarimetric variables. *Mon. Wea. Rev.*, **136**, 2228-2245.
- Jung, Y., M. Xue, and G. Zhang, 2010: Simulations of polarimetric radar signatures of a supercell storm using a two-moment bulk microphysics scheme. *J. Appl. Meteor. Climatol.*, **49**, 146-163.
- Jung, Y., M. Xue, Y. Wang, S. Wang, F. Kong, Y. Pan, and K. Zhu, 2013: Multi-Scale Ensemble Kalman Filter Data Assimilation and Forecasts in Central United States. *WMO 6th Symposium on Data Assimilation*.
- Kong, F., and Coauthors, 2007: Preliminary analysis on the real-time storm-scale ensemble forecasts produced as a part of the NOAA hazardous weather testbed 2007 spring experiment. *22nd Conf. Wea. Anal. Forecasting/18th Conf. Num. Wea. Pred.*, Salt Lake City, Utah, Amer. Meteor. Soc., CDROM 3B.2.
- Kong, F., and Coauthors, 2008: Real-time storm-scale ensemble forecast experiment - Analysis of 2008 spring experiment data. *24th Conf. Several Local Storms*, Savannah, GA, Ameri. Meteor. Soc., Paper 12.13.

- Kong, F., and Coauthors, 2009: A real-time storm-scale ensemble forecast system: 2009 Spring Experiment. *23rd Conf. Wea. Anal. Forecasting/19th Conf. Num. Wea. Pred.*, Omaha, Nebraska, Amer. Meteor. Soc., Paper 16A.13.
- Kong, F., and Coauthors, 2012: CAPS Storm-Scale Ensemble Forecasts for the NOAA 2012 HWT Spring Experiment: New Features and QPF Verification. *13th WRF Users Workshop*, Paper 5.3.
- Milbrandt, J. A., and M. K. Yau, 2006a: A multimoment bulk microphysics parameterization. Part IV: Sensitivity experiments. *Journal of the Atmospheric Sciences*, **63**, 3137-3159.
- , 2006b: A multimoment bulk microphysics parameterization. Part III: Control simulation of a hailstorm. *Journal of the Atmospheric Sciences*, **63**, 3114-3136.
- Tong, M., and M. Xue, 2005: Ensemble Kalman filter assimilation of Doppler radar data with a compressible nonhydrostatic model: OSS Experiments. *Mon. Wea. Rev.*, **133**, 1789-1807.
- Wang, Y., Y. Jung, T. A. Supinie, and M. Xue, 2013: A Hybrid MPI-OpenMP Parallel Algorithm and Performance Analysis for an Ensemble Square Root Filter Designed for Multiscale Observations. *Journal of Atmospheric and Oceanic Technology*, **30**, 1382-1397.
- Xue, M., M. Tong, and K. K. Droegemeier, 2006: An OSSE framework based on the ensemble square-root Kalman filter for evaluating impact of data from radar networks on thunderstorm analysis and forecast. *J. Atmos. Ocean Tech.*, **23**, 46-66.
- Xue, M., and Coauthors, 2007: CAPS realtime storm-scale ensemble and high-resolution forecasts as part of the NOAA Hazardous Weather Testbed 2007 spring experiment. *22nd Conf. Wea. Anal. Forecasting/18th Conf. Num. Wea. Pred.*, Amer. Meteor. Soc., CDROM 3B.1.
- Xue, M., and Coauthors, 2008: CAPS realtime storm-scale ensemble and high-resolution forecasts as part of the NOAA Hazardous Weather Testbed 2008 Spring Experiment. *24th Conf. Several Local Storms*, Savannah, GA, Amer. Meteor. Soc., Paper 12.12.
- Xue, M., and Coauthors, 2009: CAPS realtime multi-model convection-allowing ensemble and 1-km convection-resolving forecasts for the NOAA Hazardous Weather Testbed 2009 Spring Experiment. *23rd Conf. Wea. Anal. Forecasting/19th Conf. Num. Wea. Pred.*, Omaha, NB, Amer. Meteor. Soc., Paper 16A.12.
- Xue, M., and Coauthors, 2010: CAPS Realtime Storm Scale Ensemble and High Resolution Forecasts for the NOAA Hazardous Weather Testbed 2010 Spring Experiment. *25th Conf. on Severe Local Storms*, Amer. Meteor. Soc., 7B.3.
- Zhang, J., and Coauthors, 2011: National Mosaic and Multi-Sensor QPE (NMQ) System: Description, Results, and Future Plans. *Bulletin of the American Meteorological Society*, **92**, 1321-1338.